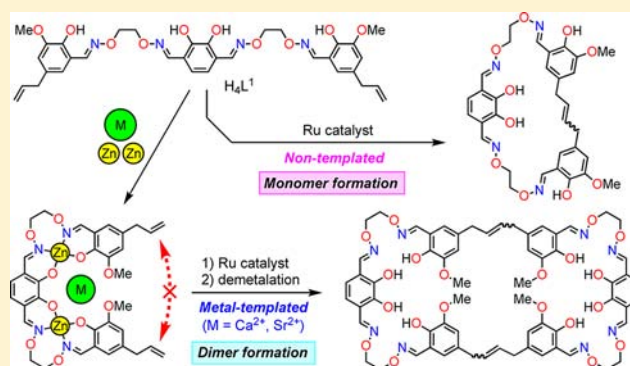


Oligometallic Template Strategy for Synthesis of a Macrocyclic Dimer-Type Octaoxime Ligand for Its Cooperative Complexation

Shigehisa Akine,^{*,†,‡} Toshio Tadokoro,[†] and Tatsuya Nabeshima^{*,†,‡}[†]Faculty of Pure and Applied Sciences and [‡]Tsukuba Research Center for Interdisciplinary Materials Science, University of Tsukuba, 1-1-1 Tennodai, Tsukuba, Ibaraki 305-8571, Japan

Supporting Information

ABSTRACT: The new acyclic tetraoxime ligand H_4L^1 , having two allyl groups at the terminal benzene rings, was designed and synthesized. The ligand H_4L^1 was converted to five kinds of the trinuclear complexes, $[L^1Zn_3(OAc)_2]$, $[L^1Zn_2La(OAc)_3]$, $[L^1Zn_2Ca(OAc)_2]$, $[L^1Zn_2Sr(OAc)_2]$, and $[L^1Zn_2Ba(OAc)_2]$. The terminal allyl groups were introduced so that the olefin metathesis could convert the metal complexes into the dimeric macrocyclic ligand H_8L^3 . The X-ray crystallographic analysis of the trinuclear complexes $[L^1Zn_3(OAc)_2(H_2O)]$, $[L^1Zn_2La(OAc)_3(MeOH)]$, $[L^1Zn_2Ca(OAc)_2]$, and $[L^1Zn_2Sr(OAc)_2]$ revealed that the distances between the two allyl groups are 11–12 Å, which should be sufficient to suppress the intramolecular reaction leading to the monomeric macrocycle H_4L^2 . Indeed, the olefin metathesis of the $[L^1Zn_2Ca(OAc)_2]$ and $[L^1Zn_2Sr(OAc)_2]$ followed by demetalation with dilute hydrochloric acid afforded the dimeric macrocycle H_8L^3 as the major product, while the reaction of the uncomplexed ligand H_4L^1 gave the monomeric macrocycle H_4L^2 as the major product. The complexation behavior of H_8L^3 at the two tetraoxime sites was investigated. Although the formation process of the hexanuclear zinc(II) complex $[L^3Zn_6]^{4+}$ was complicated, the metal exchange of the two trinuclear zinc(II) units proceeded in a two-step fashion. The analysis of the spectral changes indicated the positive and negative cooperative effects on the double metal exchange with Ca^{2+} and Ba^{2+} , respectively. The first metal exchange reactions with Ca^{2+} made the second metal exchange more favorable. Thus, the obtained dimeric macrocycle H_8L^3 has two tetraoxime coordination sites, whose complexation behavior is remotely affected by each other.



INTRODUCTION

The ring-closing olefin metathesis using ruthenium catalysts is one of the most powerful methods for obtaining cyclic organic molecules.¹ This method is useful for synthesizing various kinds of bioactive macrocycles and was sometimes employed in the final step of the synthesis of interlocked molecules.² The macrocyclization by olefin metathesis competes with polymerization as a side reaction, which is usually observed for the synthesis of various kinds of macrocycles. In general, use of a template is known to be effective to suppress the formation of the polymeric byproducts.^{3,4} Such a template effect on the ring-closing metathesis was first reported by the Grubbs group; the ring-closing metathesis of oligoethers bearing terminal allyl groups took place efficiently in the presence of a metal ion.⁵ In addition, the template metal ion affects the cis/trans ratio of the olefinic moiety of the product. We have reported the synthesis of larger macrocyclic tetraoxime derivatives on the basis of the oligometallic template strategy, in which several metal ions act as a template.^{6,7} The macrocycle showed unique multimetal complexation behavior due to the integrated chelate coordination sites.^{6b}

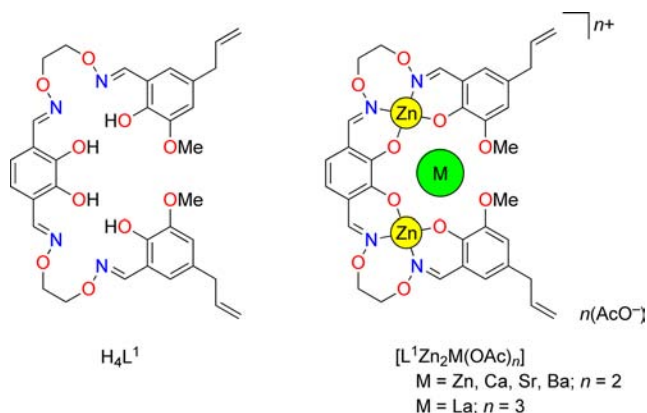
If the oligometallic template fixes the two reactive groups in such a way that they cannot intramolecularly react with each

other, only the intermolecular reaction proceeds.⁸ This would facilitate the synthesis of larger macrocycles in which more than one multimetallic core can be built. Relatively fewer examples for selective synthesis of dimeric macrocycles were reported to date.^{4a,9} Thus, we designed a new acyclic tetraoxime ligand H_4L^1 having two allyl groups at the 5-position of the terminal benzene rings (Chart 1). Upon metalation with zinc(II) and M^{n+} as a guest ion, this tetraoxime unit was expected to give a trinuclear complex $[L^1Zn_2M]^{n+}$ with a C-shaped structure.^{10–12} This makes the two allyl groups so apart from each other that the intramolecular ring-closing metathesis was suppressed even under diluted conditions. Instead, a dimeric (or larger) macrocyclic product is expected to be the major product (Scheme 1). We now report the synthesis and complexation behavior of the ligand H_4L^1 , which can be used for the selective synthesis of a dimeric macrocycle by olefin metathesis on the basis of the oligometallic template strategy. The obtained dimeric macrocycle ligand gave a zinc(II) hexanuclear complex in which each repetitive unit forms a trinuclear core. Furthermore, the hexanuclear complex underwent a unique

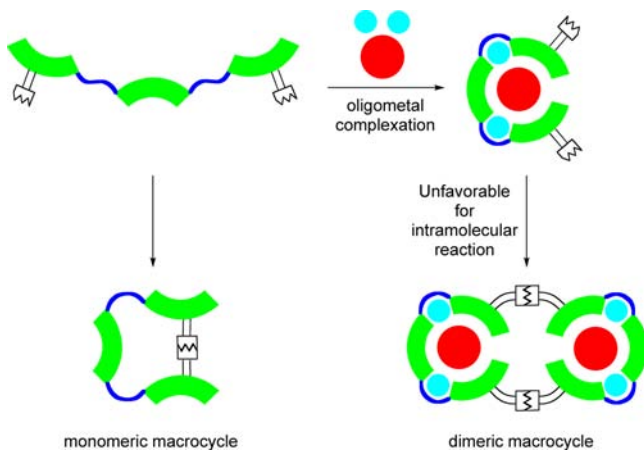
Received: June 12, 2012

Published: October 11, 2012

Chart 1



Scheme 1. Strategy for the Size-Selective Synthesis of Macrocycles under Diluted Conditions Taking Advantage of Conformational Constraint by Metal Complexation



metal exchange reaction in which the metal exchange at one trinuclear site affects that of the other site.

EXPERIMENTAL SECTION

General Procedures. All experiments were carried out in air unless otherwise noted. Dichloromethane was distilled under argon atmosphere from calcium hydride prior to use. Commercial chloroform, methanol, and ethanol were used without purification. All chemicals were of reagent grade and used as received. Column chromatography was performed with Kanto Chemical silica gel 60N (spherical, neutral). Melting points were determined on a Yanaco melting point apparatus and not corrected. 1H and ^{13}C NMR spectra were recorded on a Bruker ARX400 (400 and 100 MHz) spectrometer. Mass spectra (ESI-TOF, positive mode) were recorded on an Applied Biosystems QStar Pulsar i spectrometer. Gel permeation chromatography (GPC) was performed by an LC-908 equipped with JAIGEL 1H-2H columns (Japan Analytical Industry) with chloroform as eluent.

Materials. 2-Allyloxy-3-methoxybenzaldehyde (1),¹³ 1,2-bis-(aminoxy)ethane (3),¹⁴ and 2,3-dihydroxybenzene-1,4-dicarbaldehyde (5)^{11e,15} were synthesized according to literature. Benzylidene-[1,3-bis(2,4,6-trimethylphenyl)-2-imidazolidinylidene]dichloro-(tricyclohexylphosphine)ruthenium (Grubbs catalyst (second generation)) was purchased from Aldrich.

Synthesis of 5-Allyl-2-hydroxy-3-methoxybenzaldehyde (2). 2-Allyloxy-3-methoxybenzaldehyde (1) (5.12 g, 26.6 mmol) was placed in a test tube and heated at 215 °C for 2 h under nitrogen atmosphere. After cooling, the products were chromatographed on silica gel (eluent, hexane/ethyl acetate, 4:1) to afford rearrangement

product **2**¹⁶ (1.11 g, 22%) as yellow oil, which solidified upon cooling to give yellow crystals, mp 50–51 °C, 1H NMR (400 MHz, $CDCl_3$) δ 3.38 (dt, $J = 6.6, 1.5$ Hz, 2H), 3.91 (s, 3H), 5.11 (dq, $J = 16.8, 1.5$ Hz, 1H), 5.13 (dq, $J = 10.2, 1.5$ Hz, 1H), 5.95 (ddt, $J = 16.8, 10.2, 6.6$ Hz, 1H), 6.95 (d, $J = 1.8$ Hz, 1H), 6.99 (d, $J = 1.8$ Hz, 1H), 9.88 (s, 1H), 10.98 (s, 1H). From the crude product, 2-allyl-6-methoxyphenol (45%) and 3-allyl-4-hydroxy-5-methoxybenzaldehyde (22%) were also isolated.

Synthesis of 5-Allyl-2-hydroxy-3-methoxybenzaldehyde O-(2-(aminoxy)ethyl)oxime (4). A solution of 5-allyl-2-hydroxy-3-methoxybenzaldehyde (2) (917.6 mg, 4.77 mmol) in ethanol (90 mL) was added to a stirred solution of 1,2-bis(aminoxy)ethane (3)¹⁴ (969.4 mg, 10.5 mmol) in ethanol (40 mL) at 60 °C for a period of 30 min, and the mixture was stirred at the temperature for 1 h. After the solvent was removed under reduced pressure, the residue was subjected to column chromatography on silica gel (eluent, hexane/ethyl acetate, 1:1) and then GPC to afford monooxime **4** (1.069 g, 84%) as colorless oil, 1H NMR (400 MHz, $CDCl_3$) δ 3.32 (d, $J = 6.7$ Hz, 2H), 3.90 (s, 3H), 3.95–3.98 (m, 2H), 4.35–4.38 (m, 2H), 5.08 (dq, $J = 17.3, 1.9$ Hz, 1H), 5.08 (dq, $J = 10.7, 1.9$ Hz, 1H), 5.52 (brs, 2H), 5.94 (ddt, $J = 17.3, 10.7, 6.7$ Hz, 1H), 6.61 (d, $J = 1.9$ Hz, 1H), 6.74 (d, $J = 1.9$ Hz, 1H), 8.19 (s, 1H), 9.73 (s, 1H); ^{13}C NMR (100 MHz, $CDCl_3$) δ 39.56 (CH_2), 56.13 (CH_3), 72.66 (CH_2), 73.78 (CH_2), 113.91 (CH), 115.98 (CH_2), 116.17 (C), 121.78 (CH), 131.14 (C), 137.30 (CH), 145.33 (C), 148.05 (C), 151.56 (CH). Anal. Calcd for $C_{13}H_{18}N_2O_4$: C, 58.63; H, 6.81; N, 10.52. Found: C, 58.55; H, 6.85; N, 10.34.

Synthesis of Ligand H_4L^1 . A solution of 2,3-dihydroxybenzene-1,4-dicarbaldehyde (5)^{11e,15} (113.4 mg, 0.683 mmol) in ethanol (4 mL) was added to a stirred solution of oxime **4** (399.8 mg, 1.50 mmol) in ethanol (4 mL) at 60 °C over a period of 10 min, and the mixture was stirred at the temperature for 1 h. After cooling, the white precipitates were collected and washed with ethanol to yield ligand H_4L^1 (379.4 mg, 84%) as colorless crystals, mp 145–146 °C, 1H NMR (400 MHz, $CDCl_3$) δ 3.31 (d, $J = 6.6$ Hz, 4H), 3.89 (s, 6H), 4.47–4.52 (m, 8H), 5.07 (dq, $J = 17.3, 1.7$ Hz, 2H), 5.07 (dq, $J = 10.3, 1.7$ Hz, 2H), 5.93 (ddt, $J = 17.3, 10.3, 6.6$ Hz, 2H), 6.63 (d, $J = 1.6$ Hz, 2H), 6.73 (d, $J = 1.6$ Hz, 2H), 6.76 (s, 2H), 8.22 (s, 2H), 8.23 (s, 2H), 9.59 (s, 2H), 9.65 (s, 2H). ^{13}C NMR (100 MHz, $CDCl_3$) δ 39.56 (CH_2), 56.18 (CH_3), 73.04 (CH_2), 73.28 (CH_2), 114.08 (CH), 116.00 (CH_2), 116.07 (C), 117.59 (C), 120.80 (CH), 121.91 (CH), 131.19 (C), 137.28 (CH), 145.36 (C), 145.77 (C), 148.02 (C), 151.37 (CH), 152.05 (CH). ESI-MS observed m/z 663.2 ($[M+H]^+$); calcd for $C_{34}H_{39}N_4O_{10}$: 663.3). Anal. Calcd for $C_{34}H_{38}N_4O_{10}$: C, 61.62; H, 5.78; N, 8.45. Found: C, 61.46; H, 5.81; N, 8.38.

Synthesis of $[L^1Zn_3(OAc)_2(H_2O)]$. A solution of H_4L^1 (66.3 mg, 0.10 mmol) in chloroform (2 mL) was mixed with a solution of zinc(II) acetate dihydrate (65.9 mg, 0.30 mmol) in methanol (2 mL) at room temperature. After the solvent was removed under reduced pressure, the residue was dissolved in chloroform/methanol (1:1, 5 mL). Vapor-phase diffusion of diethyl ether into this solution yielded $[L^1Zn_3(OAc)_2(H_2O)]$ (102.8 mg, 87%) as yellow crystals. ESI-MS observed m/z 913.0 ($[L^1Zn_3(OAc)]^+$); calcd for $C_{36}H_{37}N_4O_{12}Zn_3$: 913.0). Anal. Calcd for $C_{43}H_{53}Cl_3N_4O_{16}Zn_3$ ($= [L^1Zn_3(OAc)_2(H_2O)] \cdot CHCl_3 \cdot Et_2O$): C, 43.60; H, 4.51; N, 4.73. Found: C, 43.76; H, 4.06; N, 5.25.

General Procedure for Synthesis of $[L^1Zn_2M(OAc)_n]$ ($M = La, n = 3$; $M = Ca, Sr, Ba, n = 2$). A solution of H_4L^1 (99.7 mg, 0.15 mmol) in chloroform (5 mL) was mixed with a solution of zinc(II) acetate dihydrate (65.9 mg, 0.30 mmol) in methanol (5 mL) and then a solution of $La(OAc)_3 \cdot 1.5H_2O$ or $M(OAc)_2$ ($M = Ca, Sr, Ba$) (0.15 mmol) in 50% aqueous methanol (5 mL). After the solvent was removed under reduced pressure, the residue was dissolved in chloroform/methanol (1:1, 5 mL). Vapor-phase diffusion of diethyl ether into this solution yielded the heterotrimeric complex $[L^1Zn_2M(OAc)_n]$.

$[L^1Zn_2La(OAc)_3(MeOH)]$. Orange crystals, yield 74%. ESI-MS observed m/z 1047.0 ($[L^1Zn_2La(OAc)_2]^+$); calcd for $C_{38}H_{40}LaN_4O_{14}Zn_2$: 1047.0). Anal. Calcd for $C_{43}H_{55}LaN_4O_{19}Zn_2$ ($=$

Table 1. Crystallographic Data

	[L ¹ Zn ₃ (OAc) ₂ (H ₂ O)]·CHCl ₃ ·Et ₂ O	[L ¹ Zn ₂ La(OAc) ₃ (MeOH)]·2MeOH	[L ¹ Zn ₂ Ca(OAc) ₂]·MeOH	[L ¹ Zn ₂ Sr(OAc) ₂]·2CHCl ₃
formula	C ₄₃ H ₅₃ Cl ₃ N ₄ O ₁₆ Zn ₃	C ₄₃ H ₅₅ LaN ₄ O ₁₉ Zn ₂	C ₃₉ H ₄₄ CaN ₄ O ₁₅ Zn ₂	C ₄₀ H ₄₂ Cl ₆ N ₄ O ₁₄ SrZn ₂
formula weight	1184.35	1201.56	979.60	1233.84
crystal system	triclinic	triclinic	triclinic	monoclinic
space group	P $\bar{1}$	P $\bar{1}$	P $\bar{1}$	C2/c
a (Å)	13.6167(8)	11.5253(8)	12.3350(5)	24.5784(14)
b (Å)	14.4293(8)	12.5958(7)	14.4580(5)	12.7449(7)
c (Å)	14.9773(8)	18.0527(10)	14.8059(6)	17.2856(9)
α (deg)	64.5631(14)	98.3138(15)	61.5710(10)	90
β (deg)	68.8301(16)	100.9619(18)	64.4047(14)	117.1231(19)
γ (deg)	84.4374(18)	107.4712(19)	73.0515(13)	90
V (Å ³)	2472.2(2)	2396.6(3)	2081.88(14)	4819.2(5)
Z	2	2	2	4
D _{calcd} (g cm ⁻³)	1.591	1.665	1.563	1.701
collected reflections	21600	22735	19801	22718
unique reflections	9688	10404	9028	5493
R _{int}	0.0773	0.0607	0.0331	0.0393
2θ _{max} (deg)	52.00	54.00	54.00	54.90
F ₀₀₀	1216	1220	1012	2488
μ (MoKα) (mm ⁻¹)	1.678	1.948	1.350	2.491
parameters/restraints	632/2	633/1	556/0	305/0
goodness of fit (F ²)	1.034	1.092	1.044	1.057
R1 (I > 2σ(I)) ^a	0.0615	0.0528	0.0283	0.0417
wR2 (I > 2σ(I)) ^a	0.1462	0.1060	0.0693	0.1165
R1 (all data) ^a	0.0863	0.0887	0.0360	0.0464
wR2 (all data) ^a	0.1690	0.1485	0.0744	0.1203

$$^a R1 = \sum |F_o| - |F_c| / \sum |F_o|; wR2 = [\sum w(F_o^2 - F_c^2)^2 / \sum w(F_o^2)^2]^{1/2}.$$

[L¹Zn₂La(OAc)₃(MeOH)]·2MeOH): C, 42.98; H, 4.61; N, 4.66. Found: C, 42.35; H, 4.04; N, 4.77.

[L¹Zn₂Ca(OAc)₂]. Yellow crystals, yield 78%. ESI-MS observed *m/z* 889.3 ([L¹Zn₂Ca(OAc)]⁺; calcd for C₃₆H₃₇CaN₄O₁₂Zn₂: 889.1). Anal. Calcd for C₃₉H₄₄CaN₄O₁₅Zn₂ (= [L¹Zn₂Ca(OAc)₂]·MeOH): C, 47.81; H, 4.53; N, 5.72. Found: C, 47.66; H, 4.13; N, 5.72.

[L¹Zn₂Sr(OAc)₂]. Orange crystals, yield 56%. ESI-MS observed *m/z* 935.2 ([L¹Zn₂Sr(OAc)]⁺; calcd for C₃₆H₃₇N₄O₁₂SrZn₂: 935.0). Anal. Calcd for C₃₈H₄₀N₄O₁₄SrZn₂ (= [L¹Zn₂Sr(OAc)₂]): C, 45.86; H, 4.05; N, 5.63. Found: C, 45.46; H, 4.05; N, 5.42.

[L¹Zn₂Ba(OAc)₂]. Orange crystals, yield 31%. ESI-MS observed *m/z* 985.2 ([L¹Zn₂Ba(OAc)]⁺; calcd for C₃₆H₃₇BaN₄O₁₂Zn₂: 985.0). Anal. Calcd for C_{39.5}H_{41.5}BaN₄O₁₄Zn₂ (= [L¹Zn₂Ba(OAc)₂]·1.5CHCl₃): C, 38.76; H, 3.42; N, 4.58. Found: C, 38.34; H, 3.65; N, 4.24.

General Procedure for the Ring-Closing Metathesis. A solution of Grubbs catalyst (second generation) (3.5 mg, 0.004 mmol) in dichloromethane (4 mL) was added via a transfer tube into a solution of substrate (0.040 mmol) in dichloromethane (4 mL) under nitrogen atmosphere. The solution was stirred under reflux for 72 h in the dark. The solvent was removed under reduced pressure to yield the crude product. When the metal complex was used as the substrate, the crude product was dissolved in chloroform and treated with hydrochloric acid (1 M, 12 mL), and then the organic layer was separated, dried over anhydrous magnesium sulfate, filtered, and concentrated to dryness. The mixture was treated with chloroform (3 mL), and less soluble H₈L³ was filtered if necessary. The solution was subjected to GPC, and the products (H₈L⁴, retention time 39 min; H₈L³, 42 min; H₄L¹ recovery, 44 min; H₄L², 47 min) were collected.

H₄L². Colorless crystals, mp 225–228 °C, ¹H NMR (400 MHz, CDCl₃; mixture of trans and cis isomers) trans isomer: δ 3.31 (d, *J* = 4.1 Hz, 4H), 3.89 (s, 6H), 4.47–4.54 (m, 8H), 5.61 (t, *J* = 4.1 Hz, 2H), 6.69 (d, *J* = 1.9 Hz, 2H), 6.718 (d, *J* = 1.9 Hz, 2H), 6.728 (s, 2H), 8.15 (s, 2H), 8.30 (s, 2H), 9.68 (s, 2H), 9.98 (s, 2H); cis isomer: δ 3.43 (d, *J* = 4.7 Hz, 4H), 3.90 (s, 6H), 4.47–4.54 (m, 8H), 5.66 (t, *J* = 4.7 Hz, 2H), 6.718 (d, *J* = 1.6 Hz, 2H), 6.732 (s, 2H), 6.77 (d, *J* = 1.6 Hz, 2H), 8.15 (s, 2H), 8.33 (s, 2H), 9.64 (s, 2H), 10.04 (s, 2H); ¹³C

NMR (100 MHz, CDCl₃; mixture of trans and cis isomers) trans isomer: δ 37.95 (CH₂), 56.15 (CH₃), 72.52 (CH₂), 75.91 (CH₂), 114.38 (CH), 116.18 (C), 117.60 (C), 120.79 (CH), 121.96 (CH), 130.22 (CH), 131.46 (C), 145.36 (C), 145.90 (C), 147.84 (C), 150.79 (CH), 152.16 (CH); cis isomer: δ 32.87 (CH₂), 56.15 (CH₃), 72.48 (CH₂), 76.01 (CH₂), 114.05 (CH), 116.31 (C), 117.62 (C), 120.82 (CH), 121.65 (CH), 129.31 (CH), 131.82 (C), 145.31 (C), 145.95 (C), 147.90 (C), 150.79 (CH), 152.10 (CH). ESI-MS observed *m/z* 635.3 ([M+H]⁺; calcd for C₃₂H₃₅N₄O₁₀: 635.2). Anal. Calcd for C₃₂H₃₄N₄O₁₀·H₂O: C, 58.89; H, 5.56; N, 8.58. Found: C, 58.83; H, 5.34; N, 8.47.

H₈L³. Colorless crystals, mp 195–198 °C, ¹H NMR (400 MHz, CDCl₃) δ 3.27 (d, *J* = 4.8 Hz, 8H), 3.85 (s, 12H), 4.46–4.48 (m, 16H), 5.58–5.60 (m, 4H), 6.60 (d, *J* = 1.7 Hz, 4H), 6.69 (d, *J* = 1.7 Hz, 4H), 6.72 (s, 4H), 8.19 (s, 8H), 9.52 (s, 4H), 9.65 (s, 4H); ¹³C NMR (100 MHz, DMSO-*d*₆) δ 37.49 (CH₂), 55.68 (CH₃), 71.97 (CH₂), 72.25 (CH₂), 113.56 (CH), 117.45 (CH), 117.55 (C), 117.84 (CH), 119.11 (C), 130.12 (CH), 131.32 (C), 143.74 (C), 144.96 (C), 146.36 (CH), 147.18 (CH), 147.74 (C). ESI-MS observed *m/z* 1291.5 ([M+Na]⁺; calcd for C₆₄H₆₈N₈NaO₂₀: 1291.4). Anal. Calcd for C₆₄H₆₈N₈O₂₀·4H₂O: C, 57.31; H, 5.71; N, 8.35. Found: C, 57.57; H, 5.32; N, 8.08.

H₈L⁴. Colorless solid, ¹H NMR (400 MHz, CDCl₃) trans isomer: δ 3.28 (d, *J* = 4.9 Hz, 4H), 3.31 (d, *J* = 6.8 Hz, 4H), 3.87 (s, 6H), 3.89 (s, 6H), 4.47–4.51 (br m, 16H), 5.04–5.10 (m, 4H), 5.60–5.63 (m, 2H), 5.93 (ddt, *J* = 17.4, 9.6, 6.7 Hz, 2H), 6.62 (d × 2, *J* = 1.6 Hz, 4H), 6.71 (d, *J* = 1.6 Hz, 2H), 6.73 (d, *J* = 1.6 Hz, 2H), 6.76 (s, 4H), 8.21 (s × 2, 4H), 8.23 (s × 2, 4H), 9.56 (s, 2H), 9.59 (s, 2H), 9.65 (s, 2H), 9.66 (s, 2H).

Synthesis of [L³Zn₆(OAc)₄]. A solution of H₈L³ (6.3 mg, 0.0050 mmol) in chloroform (2 mL) was mixed with a solution of zinc(II) acetate dihydrate (6.6 mg, 0.030 mmol) in methanol (2 mL). The resulting solution was heated at reflux for 4 h. The yellow precipitates were collected to give [L³Zn₆(OAc)₄] (8.2 mg, 84%) as yellow powder, ESI-MS observed *m/z* 885.1 ([L³Zn₆(OAc)₂]²⁺; calcd for C₆₈H₆₆N₈O₂₄Zn₆: 885.0), 1829.1 ([L³Zn₆(OAc)₃]⁺; calcd for C₇₀H₆₉N₈O₂₆Zn₆: 1829.0). Anal. Calcd. for C₇₂H₇₈N₈O₃₁Zn₆

($[L^3Zn_6(OAc)_4] \cdot 3H_2O$: C, 44.49; H, 4.04; N, 5.76. Found: C, 44.31; H, 3.92; N, 5.57.

1H NMR Titration ($H_8L^3-Zn^{II}$). Sample solutions containing ligand H_8L^3 (0.5 mM) and varying amounts of zinc(II) acetate dihydrate (0–10 equiv) in $CDCl_3/CD_3OD$ (1:1, 0.5 mL) were prepared. The 1H NMR spectrum (400 MHz) of each sample was recorded at 298 K.

1H NMR Titration ($H_8L^3-Zn^{II}$ -Guest Cation). Sample solutions containing ligand H_8L^3 (0.5 mM), zinc(II) acetate dihydrate (3.0 mM), and varying amounts of guest cation (Ca^{2+} , Ba^{2+} , La^{3+}) in $CDCl_3/CD_3OD$ (1:1, 0.5 mL) were prepared. The 1H NMR spectrum (400 MHz) of each sample was recorded at 298 K.

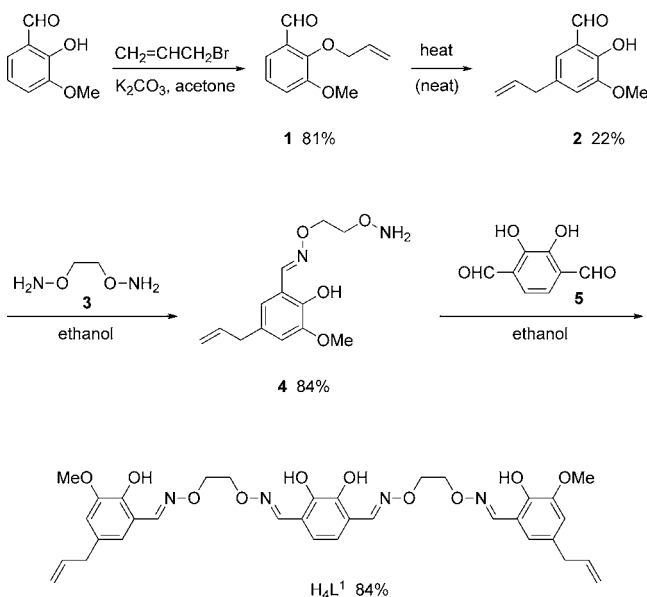
Determination of Equilibrium Constant for Metal Exchange. The mole fractions of $[L^3Zn_6]^{4+}$, $[L^3Zn_5M]^{(n+2)+}$, and $[L^3Zn_4M_2]^{2n+}$ were determined from the integral ratio of the 1H NMR spectra in the titration experiments. The changes in the mole fractions as a function of equivalents of the guest metal ion were analyzed by nonlinear least-squares regression in which two equilibrium constants, K_1 and K_2 , are variables.

X-ray Crystallography. Intensity data were collected at 120 K on a Rigaku R-Axis Rapid diffractometer with Mo $K\alpha$ radiation ($\lambda = 0.71069 \text{ \AA}$). The data were corrected for Lorentz and polarization factors, and for absorption by semiempirical methods based on symmetry-equivalent and repeated reflections. The structures were solved by Patterson methods (DIRDIF 99)¹⁷ and refined by full-matrix least-squares on F^2 using SHELXL 97.¹⁸ The crystallographic data are summarized in Table 1.

RESULTS AND DISCUSSION

Synthesis of Ligands. Ligand H_4L^1 was synthesized from allylated salicylaldehyde derivative **2**¹⁶ according to a procedure similar to that of an analogous compound without allyl groups reported previously (Scheme 2).¹¹ The allyl ether **1** was

Scheme 2. Synthesis of Ligand H_4L^1



obtained in 81% yield by the reaction of 2-hydroxy-3-methoxybenzaldehyde with allyl bromide in the presence of potassium carbonate in acetone.¹³ This compound **1** was heated at 215 °C without solvent to afford the rearranged product **2** in 22% yield.¹⁶ In this reaction, decarbonylated compound (2-allyl-6-methoxyphenol; 45%) and a formyl migration product (3-allyl-4-hydroxy-5-methoxybenzaldehyde; 22%) were also obtained. The reaction of the aldehyde **2** with excess 1,2-bis(aminooxy)ethane (**3**)¹⁴ gave monooxime **4** in

84% yield, which was then converted to the tetraoxime ligand H_4L^1 in 84% yield by condensation with 2,3-dihydroxybenzene-1,4-dicarbaldehyde (**5**)^{11e,15} in ethanol.

Synthesis and Structures of Metal Complexes. We have already reported that the complexation between the parent tetraoxime ligand without allyl groups and zinc(II) acetate gives a homotrimeric zinc(II) complex and that the complexation in the presence of a hard metal ion (La^{3+} , Ca^{2+} , Ba^{2+} , etc.) gives heterotrimeric complexes.^{11a,b,e,f} The ligand H_4L^1 has allyl groups at the opposite side of the metal coordination sites so that these allyl groups were expected to have little influence on the complexation behavior.

Indeed, the reaction of the ligand H_4L^1 with zinc(II) acetate afforded the zinc(II) trimeric complex $[L^1Zn_3(OAc)_2]$ quantitatively. The formation of the trimeric species was confirmed by the intense peak at m/z 913.0 ($= [L^1Zn_3(OAc)]^+$; calcd 913.0) in the ESI mass spectrum. This trimeric complex $[L^1Zn_3(OAc)_2]$ was isolated from the reaction mixture in 87% yield as yellow crystals. The X-ray crystallographic analysis of the complex $[L^1Zn_3(OAc)_2(H_2O)]$ (Figure 1) revealed that

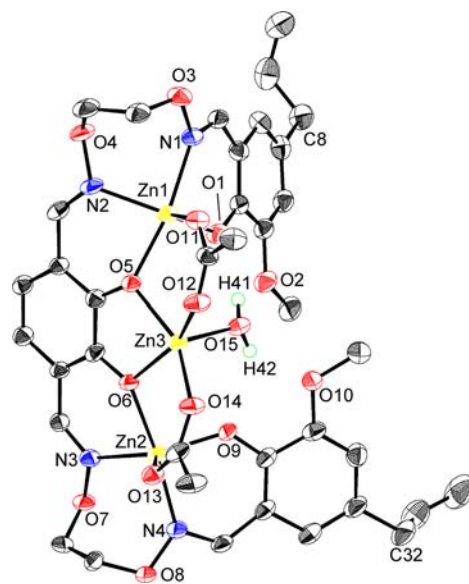


Figure 1. ORTEP drawing of $[L^1Zn_3(OAc)_2(H_2O)]$ with thermal ellipsoids plotted at 50% probability level. Hydrogen atoms except for H41 and H42 are omitted for clarity.

two of the three zinc(II) atoms (Zn1, Zn2) sit in the N_2O_2 sites and that the other (Zn3) is situated in the central O_6 site through the coordination of the catecholato moiety. The geometries of the Zn1 and Zn2 are distorted pentacoordinate trigonal bipyramidal ($\tau = 0.738, 0.668$)¹⁹ while that of the Zn3 is almost ideal square pyramidal ($\tau = 0.044$) with a water ligand (O15) at the apical position. This water molecule forms hydrogen bonds to the methoxy oxygen atoms (O15–H41...O1 and O15–H42...O10; O–O distance 2.667(5) and 2.711(5) Å, respectively). Two acetate ions coordinate to Zn1–Zn3 and Zn2–Zn3 in a bridging fashion from the same side of the molecules. This structural feature was similar to that of the parent compound without the allyl groups.^{11e} The distance between the two allylic carbon atoms (C8 and C32) is 11.3 Å, which is probably sufficient to suppress the intramolecular olefin metathesis reaction.

Heterotrimeric complexes $[L^1Zn_2M(OAc)_n]$ were prepared by the reaction of the ligand H_4L^1 with zinc(II) acetate in the

presence of metal ion M^{n+} ($= \text{La}^{3+}, \text{Ca}^{2+}, \text{Sr}^{2+}, \text{Ba}^{2+}$). The X-ray crystallographic analysis of $[\text{L}^1\text{Zn}_2\text{La}(\text{OAc})_3(\text{MeOH})]$ (Figure 2), $[\text{L}^1\text{Zn}_2\text{Ca}(\text{OAc})_2]$ (Figure 3), and $[\text{L}^1\text{Zn}_2\text{Sr}(\text{OAc})_2]$

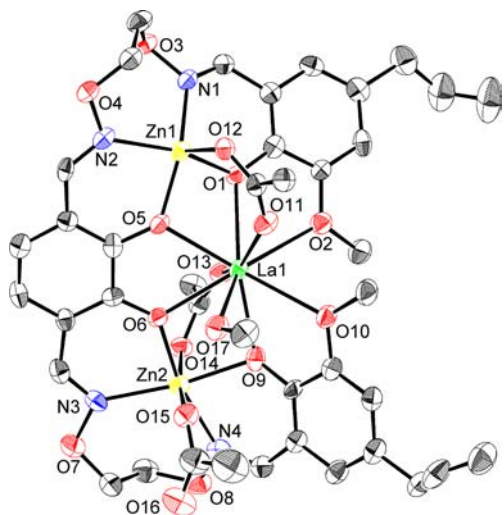


Figure 2. ORTEP drawing of $[\text{L}^1\text{Zn}_2\text{La}(\text{OAc})_3(\text{MeOH})]$ with thermal ellipsoids plotted at 50% probability level. Hydrogen atoms are omitted for clarity.

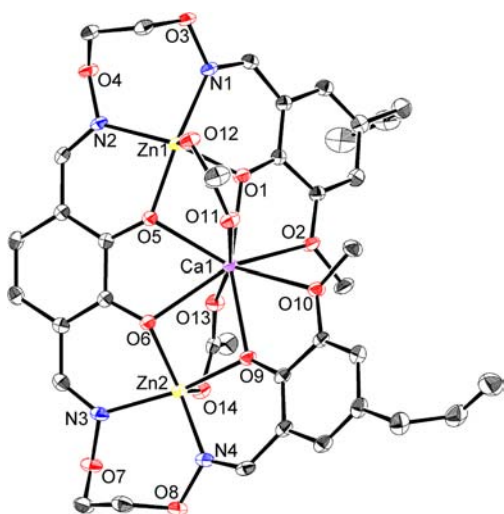


Figure 3. ORTEP drawing of $[\text{L}^1\text{Zn}_2\text{Ca}(\text{OAc})_2]$ with thermal ellipsoids plotted at 50% probability level. Hydrogen atoms are omitted for clarity.

(Figure 4) revealed that the complexes adopted a single helical structure, which is essentially the same as those of the corresponding complexes without the allyl groups.^{11e} The zinc(II) ions were in the peripheral N_2O_2 sites and adopted a pentacoordinate trigonal bipyramidal geometry except for one in $[\text{L}^1\text{Zn}_2\text{La}(\text{OAc})_3(\text{MeOH})]$. The central O_6 site was occupied by a nonacoordinate La^{3+} or an octacoordinate alkaline earth ($\text{Ca}^{2+}, \text{Sr}^{2+}$). The six oxygen donor atoms (four phenoxo and two methoxy groups) from the ligand L^{4-} coordinated to the $\text{La}^{3+}, \text{Ca}^{2+}$, or Sr^{2+} ion, fixing the L^{4-} moiety to adopt a helical structure. The formation of the coordination bonds forces the allyl groups to be directed outward and retains the allyl–allyl distances in the range of 11–12 Å. Consequently, the intramolecular olefin metathesis of

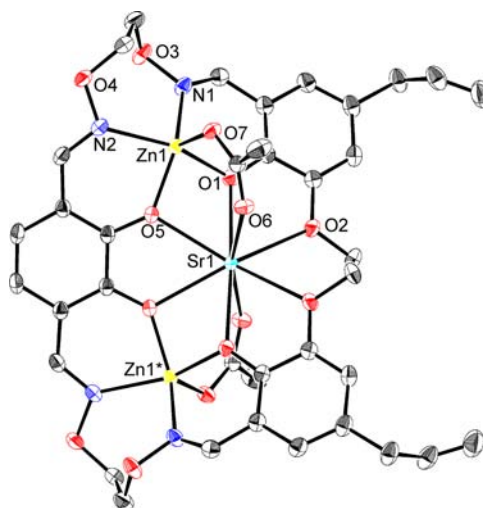


Figure 4. ORTEP drawing of $[\text{L}^1\text{Zn}_2\text{Sr}(\text{OAc})_2]$ with thermal ellipsoids plotted at 50% probability level. Hydrogen atoms are omitted for clarity.

these two allyl groups was expected to be unfavorable, while the intermolecular reaction should be favorable.

Olefin Metathesis of H_4L^1 and Its Metal Complexes.

We then investigated the metal coordination effect of conformational constraint on ring-closing olefin metathesis (RCM) (Table 2, Chart 2, Scheme 3). Treatment of the

Table 2. Ring-Closing Metathesis of H_4L^1 and Its Metal Complexes^a

entry	substrate	yield/% ^b			
		H_4L^2	H_8L^3	H_8L^4	H_4L^1 recovery
1	H_4L^1	59 [16:84]	2 [18:82]		
2	$[\text{L}^1\text{Zn}_3(\text{OAc})_2]$		2 [12:88]	9 [16:84]	47
3	$[\text{L}^1\text{Zn}_2\text{La}(\text{OAc})_3]$			6 [30:70]	53
4	$[\text{L}^1\text{Zn}_2\text{Ca}(\text{OAc})_2]$		65 [trans] ^c		
5	$[\text{L}^1\text{Zn}_2\text{Sr}(\text{OAc})_2]$		59 [trans] ^c		5
6	$[\text{L}^1\text{Zn}_2\text{Ba}(\text{OAc})_2]$		3 [13:87]	25 [18:82]	49

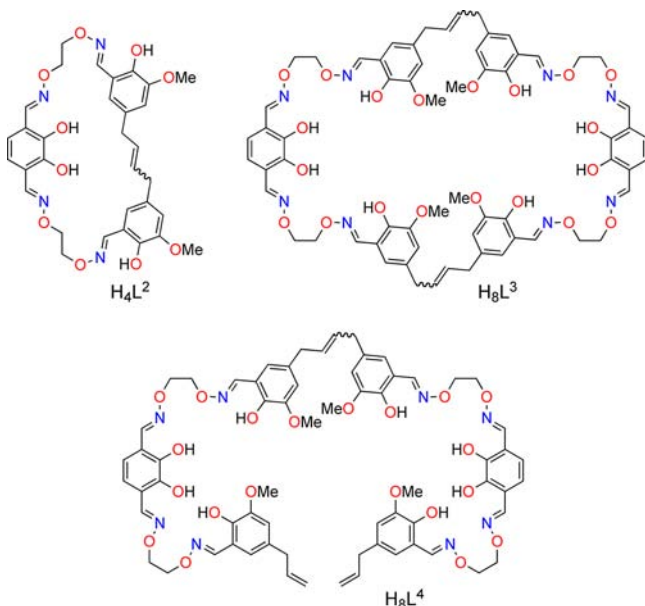
^aReaction conditions: In dichloromethane, 5 mM, 72 h, reflux, Grubbs catalyst (second generation, 10 mol %). For entries 2–6, the crude products were treated with 1 M hydrochloric acid for demetalation.

^bIsolated yields after GPC separation. The cis/trans ratios are indicated in brackets. ^cAlmost pure trans/trans isomer (>95% trans/cis).

uncomplexed ligand H_4L^1 with Grubbs catalyst (second generation) afforded an intramolecular RCM product H_4L^2 in 59% yield (Table 2, entry 1; Scheme 3, a). In addition, a small amount of dimeric macrocycle²⁰ H_8L^3 was obtained. The monomeric macrocycle H_4L^2 was obtained as a mixture of cis and trans isomers in a 16:84 ratio. The assignment of the cis and trans isomers was based on the ¹³C NMR chemical shifts²¹ of the allylic carbons (32.87 ppm for cis isomer; 37.95 ppm for trans isomer).

On the contrary, the olefin metathesis reaction of $[\text{L}^1\text{Zn}_2\text{Ca}(\text{OAc})_2]$ afforded the dimeric macrocycle as the major product. The metal-free dimeric macrocycle H_8L^3 was isolated in 65% yield after demetalation with 1 M hydrochloric acid (Table 2,

Chart 2



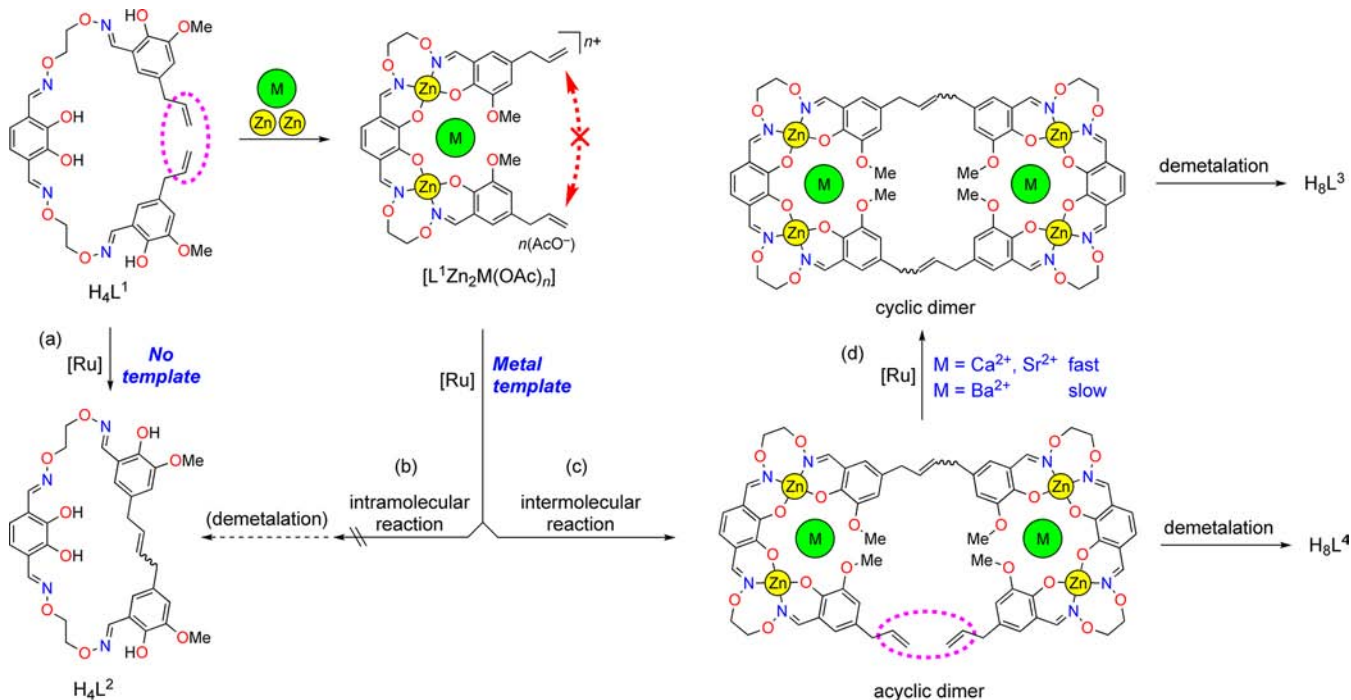
entry 4). The dimeric macrocycle H_8L^3 was obtained as the almost pure trans/trans isomer, which was confirmed by the ^{13}C NMR chemical shift of the allylic carbon at 37.49 ppm. The monomeric macrocycle H_4L^2 was not detected in the reaction mixture. Consequently, the conversion of the H_4L^1 into the Zn–Ca trinuclear complex significantly changed the selectivity and suppressed the formation of the monomeric macrocycle H_4L^2 .

The olefin metathesis of $[L^1Zn_2Sr(OAc)_2]$ similarly gave the dimeric macrocycle H_8L^3 in 59% yield after the demetalation (Table 2, entry 5). However, the olefin metathesis of other

complexes ($[L^1Zn_3(OAc)_2]$, $[L^1Zn_2La(OAc)_3]$, and $[L^1Zn_2Ba(OAc)_2]$) gave the dimeric macrocycle H_8L^3 in low yields (entries 2, 3, and 6). In these cases, the crude reaction mixture after demetalation mainly contained the recovered starting material H_4L^1 in addition to a small amount of acyclic dimer H_8L^4 and the dimeric macrocycle H_8L^3 .

The formation of the monomeric macrocycle H_4L^2 was completely suppressed (Scheme 3, b) when the metal complexes were used as a substrate. This is because the metal coordination fixes the two terminal allyloxy groups so far that they cannot undergo the olefin metathesis reaction in an intramolecular fashion. Instead, intermolecular reaction took place to give the acyclic dimer (Scheme 3, c). It is interesting to note that the yield of the dimeric macrocycle H_8L^3 significantly depends on the substrate complexes. Among the complexes containing alkaline earth metal ions, $[L^1Zn_2M(OAc)_2]$ ($M = Ca, Sr$) gave the dimeric macrocycle H_8L^3 in a higher yield (Scheme 3, d) while $[L^1Zn_2Ba(OAc)_2]$ having a larger Ba^{2+} ion gave the acyclic dimer H_8L^4 in a low yield. In contrast, the reaction of $[L^1Zn_3(OAc)_2]$ and $[L^1Zn_2La(OAc)_3]$ yielded the metathesis products (H_8L^3 and H_8L^4) in very low yield. As a result, the Zn–Ca and Zn–Sr were suitable combinations for selectively obtaining the dimeric macrocycle H_8L^3 .

The reason why $[L^1Zn_2Ba(OAc)_2]$ gave the dimeric macrocycle H_8L^3 in a lower yield than $[L^1Zn_2Ca(OAc)_2]$ and $[L^1Zn_2Sr(OAc)_2]$ can be explained by the larger ionic radius of Ba^{2+} that possibly causes a steric strain in the macrocyclic product. However, $[L^1Zn_2La(OAc)_3]$ gave the macrocyclic product H_8L^3 in low yields, although La^{3+} has an ionic radius not so different from those of Ca^{2+} or Sr^{2+} . Obviously, the ionic radius of the central metal ion (La^{3+} , Ca^{2+} , Sr^{2+} , and Ba^{2+}) was not the sole factor in determining the yield of H_8L^3 . Since the olefin metathesis reaction of $[L^1Zn_2La(OAc)_3]$ or $[L^1Zn_3(OAc)_2]$ did not proceed efficiently, the trinuclear core

Scheme 3. Olefin Metathesis of H_4L^1 and Its Metal Complexes^a

^a[Ru] = Grubbs catalyst (second generation).

of these complexes presumably deactivated the Grubbs catalyst under the reaction conditions.

Complexation Behavior of the Cyclic Ligands. We have already reported that the complexation of a tetraoxime ligand with zinc(II) gave a homotrimeric complex and that the metal exchange of the complex afforded heterotrimeric complexes.^{11a,b,e} In the case of the dimeric macrocyclic ligand H_8L^3 , the two tetraoxime moieties might affect each other in the complexation behavior. We investigated the complexation behavior of the dimeric macrocycle H_8L^3 with zinc(II) acetate in comparison with that of the acyclic analogue H_4L^1 .

The 1H NMR titration experiments showed that the complexation of the allylated ligand H_4L^1 with zinc(II) acetate took place highly cooperatively to afford homotrimeric complex $[L^1Zn_3]^{2+}$ as observed for the previously reported ligand without allyloxy groups.^{11a,b,e} Similarly, the dimeric macrocyclic ligand H_8L^3 formed a homo-hexanuclear complex $[L^3Zn_6]^{4+}$ upon the addition of 6 equiv of zinc(II) acetate (Figure 5). The formation of the hexanuclear species $[L^3Zn_6]^{4+}$

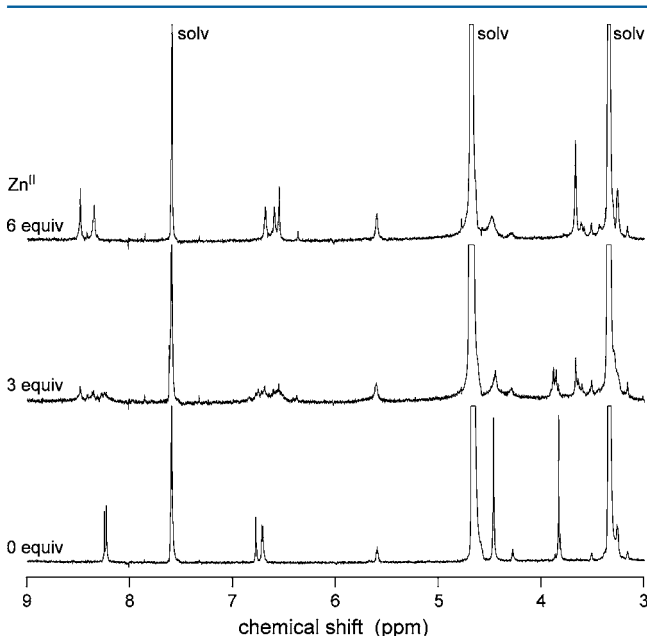


Figure 5. 1H NMR spectral changes in H_8L^3 (400 MHz, 0.5 mM) in $CDCl_3/CD_3OD$ (1:1) upon the addition of zinc(II) acetate.

was confirmed by the mass spectrum showing peaks at m/z 885.1 for $[L^3Zn_6(OAc)_2]^{2+}$ (calcd 885.0) and 1829.1 for $[L^3Zn_6(OAc)_3]^+$ (calcd 1829.0). However, in the presence of 3 equiv of zinc(II), the 1H NMR spectrum showed several signals that can be assigned to the intermediate species. This indicates that the complexation with 6 equiv of zinc(II) ions did not take place cooperatively.

We have already reported that the homotrimeric zinc(II) complex of the parent acyclic ligand undergoes quantitative metal exchange with La^{3+} , Ca^{2+} , and so forth.^{11e} In a similar manner, the metal exchange of $[L^3Zn_6]^{4+}$ having two trimeric cores with guest ions was investigated by spectroscopic methods. When Ca^{2+} was added to a solution of $[L^3Zn_6]^{4+}$, two sets of signals appeared separately from that of the $[L^3Zn_6]^{4+}$ (Figure 6). The signals were assigned to hetero-hexanuclear complexes $[L^3Zn_5Ca]^{4+}$ and $[L^3Zn_4Ca_2]^{4+}$. The addition of more than 3 equiv of Ca^{2+} resulted in the disappearance of the signals of $[L^3Zn_6]^{4+}$ and the exclusive

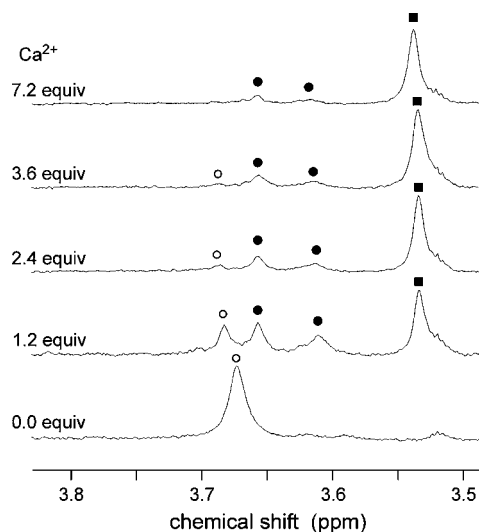


Figure 6. Part of the 1H NMR spectra of $[L^3Zn_6]^{4+}$ (400 MHz, 0.5 mM) in the presence of varying amounts of $Ca(NO_3)_2$ in $CDCl_3/CD_3OD$ (1:1). The open circles, filled circles, and filled squares denote the signals of the methoxy groups for $[L^3Zn_6]^{4+}$, $[L^3Zn_5Ca]^{4+}$, and $[L^3Zn_4Ca_2]^{4+}$, respectively.

formation of $[L^3Zn_4Ca_2]^{4+}$. The double metal exchange from $[L^3Zn_6]^{4+}$ to $[L^3Zn_4Ca_2]^{4+}$ was confirmed by the mass spectrum, showing the heterometallic species containing four Zn^{2+} and two Ca^{2+} ions (m/z 1779.0 for $[L^3Zn_4Ca_2(OAc)_3]^+$ (calcd 1779.1), 860.0 for $[L^3Zn_4Ca_2(OAc)_2]^{2+}$ (calcd 860.0), 553.7 for $[L^3Zn_4Ca_2(OAc)]^{3+}$ (calcd 553.7), and 400.5 for $[L^3Zn_4Ca_2]^{4+}$ (calcd 400.5)). The metal exchange similarly took place when La^{3+} was added. When 1 equiv of La^{3+} was added to $[L^3Zn_6]^{4+}$, the spectra showed signals for three species, which can be assigned to $[L^3Zn_6]^{4+}$, $[L^3Zn_5La]^{5+}$, and $[L^3Zn_4La_2]^{6+}$. However, 2 equiv of La^{3+} were sufficient to completely change $[L^3Zn_6]^{4+}$ into $[L^3Zn_4La_2]^{6+}$. The formation of $[L^3Zn_4La_2]^{6+}$ was confirmed by the mass spectrum (m/z 1018.0 for $[L^3Zn_4La_2(OAc)_4]^{2+}$ (calcd 1018.0), 659.0 for $[L^3Zn_4La_2(OAc)_3]^{3+}$ (calcd 659.0), and 479.5 for $[L^3Zn_4La_2(OAc)_2]^{4+}$ (calcd 479.5)).

In the double metal exchange process of $[L^3Zn_6]^{4+}$, the first metal exchange at one trimeric core might cause a structural change in the other site, which would more or less affect the efficiency of the second metal exchange. This situation is closely related to the cooperative host–guest complexation in a two-site receptor.²² If the first metal exchange enhances (or suppresses) the second metal exchange, the process is positively (or negatively) cooperative.

The equilibrium constants (K_1 and K_2) for the two-step metal exchange (Scheme 4) were determined by nonlinear least-squares regression of the mole fractions (Table 3). The cooperativity can be analyzed in a way similar to the cooperative host–guest complexation; condition $4K_2/K_1 > 1$ corresponds to positive cooperativity.²³ The $4K_2/K_1$ value for double metal exchange with Ca^{2+} was 4.8, indicative of positive cooperativity. The first metal exchange with Ca^{2+} makes the second metal exchange more favorable. On the other hand, the $4K_2/K_1$ value for Ba^{2+} was 0.26, which indicates negative cooperativity. In the case of La^{3+} ($4K_2/K_1 \sim 0.8$), the first and the second metal exchange proceeded almost independently, indicative of little cooperative effect.

The larger $4K_2/K_1$ value for Ca^{2+} suggests that the first metal exchange with Ca^{2+} changes the structure of $[L^3Zn_6]^{4+}$ to

Scheme 4. Equilibria for Stepwise Metal Exchange of $[L^3Zn_6]^{4+}$ with a Guest Metal Ion M^{n+}

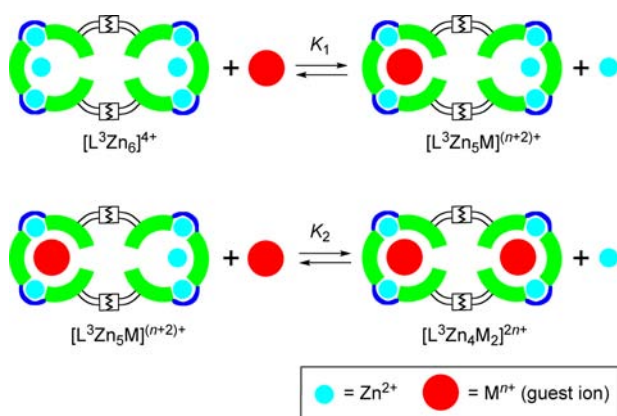


Table 3. Equilibrium Constants K_1 and K_2 for Double Metal Exchange^a

guest ^b	K_1	K_2	$4K_2/K_1$	cooperativity
Ca ²⁺	6.0(8)	7.3(4)	4.8	positive
Ba ²⁺	1.3(1)	0.087(8)	0.26	negative
La ³⁺	c	c	0.8 ^d	

^aDetermined by ¹H NMR spectroscopy. Concentration of $[L^3Zn_6]^{4+}$, 0.5 mM, CDCl₃/CD₃OD (1:1). ^bCa(NO₃)₂, Ba(OTf)₂, and La(OTf)₃ were used as the guest. ^cThe equilibrium constants for each step were too large to be accurately determined. ^dThe $4K_2/K_1$ value was roughly estimated from the mole fractions of $[L^3Zn_6]^{4+}$, $[L^3Zn_5La]^{5+}$, and $[L^3Zn_4La_2]^{6+}$ in the solution of $[L^3Zn_6]^{4+}$ in the presence of 1 equiv of La³⁺.

become more favorable for the second metal exchange. The macrocyclic framework with 2-butenylene linkers between the two tetraoxime units is suitable for incorporation of two Zn₂Ca cores simultaneously. In the case of the metal exchange with Ba²⁺, however, the second complexation is less favorable than that of the first step. This is probably because the first metal exchange with the larger Ba²⁺ ion at one tetraoxime moiety unfavorably distorts the other Zn₃ core or the double metal exchange product $[L^3Zn_4Ba_2]^{4+}$ is more strained than the monoexchanged product $[L^3Zn_5Ba]^{4+}$. Thus, the favorable formation of $[L^3Zn_4Ca_2]^{4+}$ in the complexation study is consistent with the fact that the Zn₂Ca core gave this dimeric macrocycle H₈L³ in higher yield than the Zn₂Ba core in the ring-closing olefin metathesis.

CONCLUSION

The new acyclic tetraoxime ligand H₄L¹, having two allyl groups at the terminal benzene rings, was designed and synthesized. The ligand H₄L¹ was converted to five kinds of the trinuclear complexes, $[L^1Zn_3(OAc)_2]$, $[L^1Zn_2La(OAc)_3]$, $[L^1Zn_2Ca(OAc)_2]$, $[L^1Zn_2Sr(OAc)_2]$, and $[L^1Zn_2Ba(OAc)_2]$. The X-ray crystallographic analysis of the trinuclear complexes $[L^1Zn_3(OAc)_2(H_2O)]$, $[L^1Zn_2La(OAc)_3(MeOH)]$, $[L^1Zn_2Ca(OAc)_2]$, and $[L^1Zn_2Sr(OAc)_2]$ revealed that the distances between the two allyl groups are in the range of 11–12 Å. The olefin metathesis of the $[L^1Zn_2Ca(OAc)_2]$ and $[L^1Zn_2Sr(OAc)_2]$ followed by demetalation with dilute hydrochloric acid afforded the dimeric macrocycle H₈L³ as the major product, while the reaction of the uncomplexed ligand H₄L¹ gave the monomeric macrocycle H₄L² as the major product. Thus, the conversion of the H₄L¹ into the Zn–Ca or Zn–Sr trinuclear

complexes significantly constrains the conformation of the two allyl groups so that the formation of the monomeric macrocycle H₄L² was completely suppressed. The complexation of the obtained dimeric macrocycle H₈L³ with 6 equiv of zinc(II) ions afforded a hexanuclear zinc(II) complex $[L^3Zn_6]^{4+}$ that has two trinuclear cores. The metal exchange of the two trinuclear zinc(II) units with a guest ion (Ca²⁺, Ba²⁺, La³⁺) proceeded in a two-step fashion. The analysis of the spectral changes indicated the positive and negative cooperativity for the double metal exchange with Ca²⁺ and Ba²⁺, respectively. The first metal exchange reactions with Ca²⁺ (or Ba²⁺) makes the second metal exchange more (or less) favorable. Therefore, the metal exchange behavior of the two trinuclear zinc(II) units was remotely affected by each other.

The synthetic strategy for dimeric macrocyclic ligands using metal complexation is useful for obtaining metal complexes having two or more multimetallic cores. Such multimetallic complexes would serve as a cooperative and cascade-type multifunctional molecule in which multiple functions such as catalytic activity, magnetic or photophysical properties, and so forth are controlled by mutual interactions between the metal cores.

ASSOCIATED CONTENT

Supporting Information

X-ray crystallographic data in CIF format. This material is available free of charge via the Internet at <http://pubs.acs.org>.

AUTHOR INFORMATION

Corresponding Author

*E-mail: akine@chem.tsukuba.ac.jp (S.A.), nabesima@chem.tsukuba.ac.jp (T.N.).

Notes

The authors declare no competing financial interest.

ACKNOWLEDGMENTS

This work was supported by Grants-in-Aid for Scientific Research from the Ministry of Education, Culture, Sports, Science and Technology, Japan.

REFERENCES

- (1) For reviews, see: (a) Trnka, T. M.; Grubbs, R. H. *Acc. Chem. Res.* **2001**, *34*, 18–29. (b) Grubbs, R. H. *Tetrahedron* **2004**, *60*, 7117–7140. (c) Grubbs, R. H. *Angew. Chem., Int. Ed.* **2006**, *45*, 3760–3765.
- (2) (a) Dietrich-Buchecker, C.; Rapenne, G.; Sauvage, J.-P. *Coord. Chem. Rev.* **1999**, *185–186*, 167–176. (b) Aricó, F.; Badjic, J. D.; Cantrill, S. J.; Flood, A. H.; Leung, K. C.-F.; Liu, Y.; Stoddart, J. F. *Top. Curr. Chem.* **2005**, *249*, 203–259. (c) Dietrich-Buchecker, C.; Jimenez-Molero, M. C.; Sartor, V.; Sauvage, J.-P. *Pure Appl. Chem.* **2003**, *75*, 1383–1393. (d) Molokanova, O.; Bogdan, A.; Vysotsky, M. O.; Bolte, M.; Ikai, T.; Okamoto, Y.; Böhmer, V. *Chem.—Eur. J.* **2007**, *13*, 6157–6170.
- (3) Anderson, S.; Anderson, H. L.; Sanders, J. K. M. *Acc. Chem. Res.* **1993**, *26*, 469–475.
- (4) For template-directed ring-closing metathesis, see: (a) Clark, T. D.; Ghadiri, M. R. *J. Am. Chem. Soc.* **1995**, *117*, 12364–12365. (b) Ng, P. L.; Lambert, J. N. *Synlett* **1999**, 1749–1750. (c) Cardullo, F.; Calama, M. C.; Snellink-Ruël, B. H. M.; Weidmann, J.-L.; Bielejewska, A.; Fokkens, R.; Nibbering, N. M. M.; Timmerman, P.; Reinhoudt, D. N. *Chem. Commun.* **2000**, 367–368. (d) Chuchuryukin, A. V.; Dijkstra, H. P.; Suijkerbuijk, B. M. J. M.; Klein Gebbink, R. J. M.; van Klink, G. P. M.; Mills, A. M.; Spek, A. L.; van Koten, G. *Angew. Chem., Int. Ed.* **2003**, *42*, 228–230. (e) Yang, X.; Gong, B. *Angew. Chem., Int. Ed.* **2005**, *44*, 1352–1356. (f) Kaucher, M. S.; Harrell, W. A., Jr.; Davis, J.

- T. *J. Am. Chem. Soc.* **2006**, *128*, 38–39. (g) Nawara, A. J.; Shima, T.; Hampel, F.; Gladysz, J. A. *J. Am. Chem. Soc.* **2006**, *128*, 4962–4963. (h) Hiraoka, S.; Yamauchi, Y.; Arakane, R.; Shionoya, M. *J. Am. Chem. Soc.* **2009**, *131*, 11646–11647.
- (5) Marsella, M. J.; Maynard, H. D.; Grubbs, R. H. *Angew. Chem., Int. Ed. Engl.* **1997**, *36*, 1101–1103.
- (6) (a) Akine, S.; Kagiya, S.; Nabeshima, T. *Inorg. Chem.* **2007**, *46*, 9525–9527. (b) Akine, S.; Kagiya, S.; Nabeshima, T. *Inorg. Chem.* **2010**, *49*, 2141–2152.
- (7) For related oligometallic template synthesis, see: (a) Akine, S.; Sunaga, S.; Taniguchi, T.; Miyazaki, H.; Nabeshima, T. *Inorg. Chem.* **2007**, *46*, 2959–2961. (b) Akine, S.; Sunaga, S.; Nabeshima, T. *Chem.—Eur. J.* **2011**, *17*, 6853–6861. (c) Nabeshima, T.; Miyazaki, H.; Iwasaki, A.; Akine, S.; Saiki, T.; Ikeda, C. *Tetrahedron* **2007**, *63*, 3328–3333. (d) Yamashita, A.; Watanabe, A.; Akine, S.; Nabeshima, T.; Nakano, M.; Yamamura, T.; Kajiura, T. *Angew. Chem., Int. Ed.* **2011**, *50*, 4016–4019.
- (8) (a) Haak, R. M.; Belmonte, M. M.; Escudero-Adán, E. C.; Benet-Buchholz, J.; Kleij, A. W. *Dalton Trans.* **2010**, *39*, 593–602. (b) Haak, R. M.; Castilla, A. M.; Belmonte, M. M.; Escudero-Adán, E. C.; Benet-Buchholz, J.; Kleij, A. W. *Dalton Trans.* **2011**, *40*, 3352–3364.
- (9) For example, see: (a) Arakawa, K.; Eguchi, T.; Kakinuma, K. *J. Org. Chem.* **1998**, *63*, 4741–4745. (b) Rapenne, G.; Dietrich-Buchecker, C.; Sauvage, J.-P. *J. Am. Chem. Soc.* **1999**, *121*, 994–1001.
- (10) For reviews, see: (a) Akine, S.; Nabeshima, T. *Dalton Trans.* **2009**, 10395–10408. (b) Akine, S. *J. Inclusion Phenom. Macrocycl. Chem.* **2012**, *72*, 25–54.
- (11) (a) Akine, S.; Taniguchi, T.; Nabeshima, T. *Angew. Chem., Int. Ed.* **2002**, *41*, 4670–4673. (b) Akine, S.; Taniguchi, T.; Saiki, T.; Nabeshima, T. *J. Am. Chem. Soc.* **2005**, *127*, 540–541. (c) Akine, S.; Matsumoto, T.; Taniguchi, T.; Nabeshima, T. *Inorg. Chem.* **2005**, *44*, 3270–3274. (d) Akine, S.; Taniguchi, T.; Nabeshima, T. *Tetrahedron Lett.* **2006**, *47*, 8419–8422. (e) Akine, S.; Taniguchi, T.; Nabeshima, T. *J. Am. Chem. Soc.* **2006**, *128*, 15765–15774. (f) Akine, S.; Taniguchi, T.; Nabeshima, T. *Inorg. Chem.* **2008**, *47*, 3255–3264.
- (12) For related complexes, see: (a) Akine, S.; Taniguchi, T.; Matsumoto, T.; Nabeshima, T. *Chem. Commun.* **2006**, 4961–4963. (b) Akine, S.; Matsumoto, T.; Nabeshima, T. *Chem. Commun.* **2008**, 4604–4606. (c) Akine, S.; Hotate, S.; Matsumoto, T.; Nabeshima, T. *Chem. Commun.* **2011**, *47*, 2925–2927. (d) Akine, S.; Matsumoto, T.; Sairenji, S.; Nabeshima, T. *Supramol. Chem.* **2011**, *23*, 106–112. (e) Akine, S.; Hotate, S.; Nabeshima, T. *J. Am. Chem. Soc.* **2011**, *133*, 13868–13871.
- (13) Kim, E.; Kim, J. Y.; Rhee, H. *Bull. Korean Chem. Soc.* **2004**, *25*, 1720–1722.
- (14) Dixon, D. W.; Weiss, R. H. *J. Org. Chem.* **1984**, *49*, 4487–4494.
- (15) Akine, S.; Taniguchi, T.; Nabeshima, T. *Tetrahedron Lett.* **2001**, *42*, 8861–8864.
- (16) (a) Molina, P.; Alajarin, M.; Vidal, A. *J. Org. Chem.* **1990**, *55*, 6140–6147. (b) Kilényi, S. N.; Mahaux, J.-M.; Van Durme, E. *J. Org. Chem.* **1991**, *56*, 2591–2594. (c) Mali, R. S.; Massey, A. P. *J. Chem. Res. (S)* **1998**, 230–231.
- (17) Beurskens, P. T.; Beurskens, G.; de Gelder, R.; Garcia-Granda, S.; Gould, R. O.; Israel, R.; Smits, J. M. M. *The DIRDIF-99 Program system*; Crystallography Laboratory, University of Nijmegen: Nijmegen, The Netherlands, 1999.
- (18) SHELXL 97, program for crystal structure refinement; Sheldrick, G. M. *Acta Crystallogr., Sect. A* **2008**, *64*, 112–122.
- (19) The trigonality index τ ($\tau = 0$ denotes ideal square pyramidal; $\tau = 1$ denotes ideal trigonal bipyramidal) was calculated according to the literature. See: Addison, A. W.; Rao, T. N.; Reedijk, J.; van Rijn, J.; Verschoor, G. C. *J. Chem. Soc., Dalton Trans.* **1984**, 1349–1356.
- (20) In this paper, we refer to H_8L^3 and H_8L^4 as dimeric macrocycle and acyclic dimer, respectively, which are obtained by olefin metathesis of two H_4L^1 molecules with the loss of one or two ethylene molecules.
- (21) For assignment of cis/trans geometry of olefins by ^{13}C NMR chemical shifts, see: (a) Pfeffer, P. E.; Luddy, F. E.; Unruh, J.; Shoolery, J. N. *J. Am. Oil Chem. Soc.* **1977**, *54*, 380–386. (b) Heathcock, C. H.; Buse, C. T.; Kleschick, W. A.; Pirrung, M. C.; Sohn, J. E.; Lampe, J. *J. Org. Chem.* **1980**, *45*, 1066–1081. (c) Gunstone, F. D. *J. Am. Oil Chem. Soc.* **1993**, *70*, 965–970.
- (22) (a) Perutz, M. F. *Q. Rev. Biophys.* **1989**, *22*, 139–237. (b) Hunter, C. A.; Anderson, H. L. *Angew. Chem., Int. Ed.* **2009**, *48*, 7488–7499.
- (23) Rebek, J., Jr.; Costello, T.; Marshall, L.; Wattle, R.; Gadwood, R. C.; Onan, K. *J. Am. Chem. Soc.* **1985**, *107*, 7481–7487.